Development of Ultra-High Strength Cold-Rolled Martensitic Steel

PEI-HENG LIU*, TSO-FENG WU and PO-CHENG HSIEH*****

**Iron and Steel Research & Development Department*
***Metallurgical Department*
****Rolling Mill Department Ⅲ*
China Steel Corporation

To address the increasing demand for lightweight and high-strength materials in the automotive industry, this study focuses on the development of a cold-rolled martensitic steel using 15B36 as the base material. A series of laboratory simulations was conducted to optimize key thermal processing parameters. Continuous Cooling Transformation (CCT) analysis identified a critical cooling rate of 16°C/s and a martensite start (Ms) temperature of approximately 340°C. Experimental results demonstrated that reducing the cooling rate from 40°C/s to 20°C/s led to a moderate decrease in tensile strength of about 30 MPa. In contrast, tempering conditions showed more pronounced effects: lowering the tempering temperature from 320°C to 260°C increased the tensile strength by approximately 270 MPa. However, prolonged tempering at lower temperatures led to a strength loss of around 60 MPa, indicating potential over-tempering or tempering embrittlement. Microstructural characterization using OM and SEM revealed a fully martensitic matrix with varying degrees of auto-tempering, depending on the processing route. These findings provide valuable insights into the heat-treatment design for 15B36. Future work will focus on enhancing formability and expanding the feasible thickness range to meet broader application requirements in structural components.

Keywords: Ultra-high-strength steels (UHSS), Martensitic steels, Auto-tempering

1. INTRODUCTION

In response to the growing demand for lightweight and high-strength automotive components, particularly from the electric vehicle sector, the development of ultra-high-strength steel (UHSS) has become increasingly essential. This study focuses on the development of a cold-rolled martensitic steel with tensile strength exceeding 1500 MPa, suitable for structural parts such as bumper reinforcements.

The target material was developed using 15B36 steel through laboratory trials and production-line simulations, aiming to meet performance requirements while enhancing domestic supply capabilities. Martensitic steels, traditionally used in hot-stamping applications, have seen rising demand in cold-formed automotive parts due to advancements in forming technology.

Components such as bumper beams, pillar and door reinforcements, as well as electric vehicle battery cases, benefit from the high strength and lightweight potential of cold-rolled martensitic steels. According to industry reports, domestic demand for MS1300-MS1500 grades has grown steadily.

Martensitic steels are characterized by their exceptional strength, which stems from their non-diffusional transformation from austenite. This transformation significantly increases dislocation density, enabling high strength that can be further enhanced through controlled tempering. Recent developments in process control have enabled the effective use of boron steels in cold-rolled applications. Critical factors influencing martensitic formation include alloy composition, cooling rate, and austenite grain size.

The hardenability of steel is primarily influenced by its chemical composition and grain size. Elements such as carbon (C), manganese (Mn), chromium (Cr), molybdenum (Mo), and boron (B) are particularly effective in increasing hardenability. These elements shift the Continuous Cooling Transformation (CCT) curves to the right side, thereby lowering the critical cooling rate needed to form martensite. This adjustment is especially valuable in continuous processing lines where rapid cooling may be constrained. Among these, boron is known for its strong hardenability enhancement at very low concentrations by segregating to austenite grain boundaries and retarding the nucleation of proeutectoid

ferrite. Manganese and chromium delay the formation of pearlite and bainite, further extending the time available for martensitic transformation. Additionally, austenite grain coarsening reduces nucleation sites for softer transformation products, thus favoring martensite formation over a broader range of processing conditions.

In addition to hardenability, alloying elements also affect the martensitic start temperature (Ms). Most alloying elements, except aluminum, tend to lower the Ms temperature, with carbon having the most significant influence. While alloy additions reduce the critical cooling rate for martensite formation, they also lower the Ms temperature. The combined effects of these two factors can either benefit or challenge the production line's cooling capability, making experimental validation essential.

Auto-tempering, or partial tempering of martensite during slow cooling or in thick sections, plays a vital role in balancing strength and ductility. This phenomenon occurs when martensite forms at relatively high temperatures, typically just below the Ms temperature. At these elevated temperatures, carbon atoms in the supersaturated martensitic matrix have enough mobility to diffuse and form fine carbides, leading to a tempered martensite structure without a distinct tempering stage. Moderate auto-tempering helps relieve internal stresses and suppress the formation of brittle, untempered martensite, thereby improving yield strength and toughness. However, excessive tempering during slow cooling can lead to over-aging effects, such as carbide coarsening and matrix softening, ultimately reducing both strength and ductility. Figure 1 presents a schematic representation of auto-tempering during continuous cooling, where martensite begins to form below the Ms temperature.

Studies have shown that the extent of auto-tempering is influenced by carbon content and cooling rate. Higher-carbon steels tend to exhibit less auto-tempering due to a lower Ms temperature, while low-carbon boron steels like 15B36 are more prone to auto-tempering, especially under moderate cooling rates. Microstructure analysis can reveal the extent of carbide precipitation and dislocation recovery, serving as indicators of auto-tempering distribution and intensity. Recent developments in cold-rolled martensitic steels have utilized controlled cooling and advanced furnace configurations to achieve a fully martensitic structure with tailored properties. The manipulation of Ms temperature and tempering control are key strategies.

2. EXPERIMENTAL METHOD

The steel development began with the construction of a Continuous Cooling Transformation (CCT) diagram for 15B36 to understand critical cooling rates and the martensite start (Ms) temperature. Samples were prepared for dilatometer testing, and the schematic diagram is shown in Figure 2a. The specimens were heated to 880°C and held for 3 minutes before being quenched at various cooling rates ranging from 1 to 100°C/s. The resulting dilation curves were analyzed to construct the CCT diagram.

Following the determination of the critical cooling rate and Ms temperature for 15B36, continuous annealing simulations were conducted. The experimental simulations included variations in cooling rates and tempering temperatures to assess their influence on martensitic transformation and subsequent auto-tempering behavior.

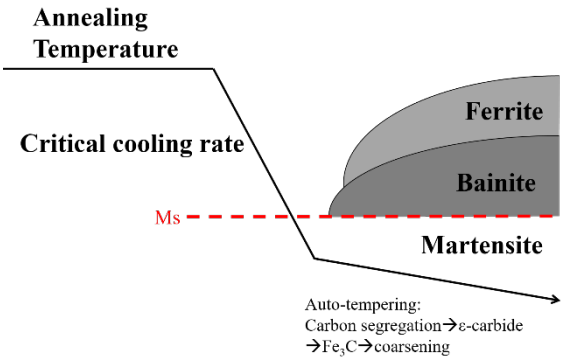

Fig.1. Schematic of auto-tempered martensite during continuous cooling.

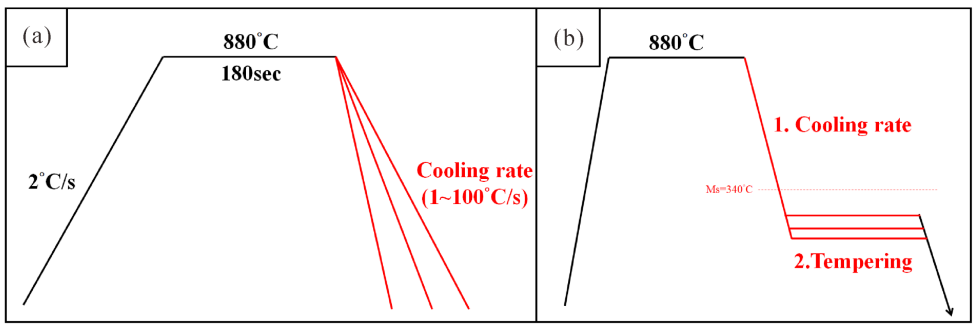

Fig.2. Schematic diagram of (a) dilatometer experiment for CCT curve and (b) simulated continuous annealing experiments.

Figure 2b illustrates the schematic diagram used in the continuous annealing experiments with the parameters of cooling rates and tempering conditions. The tempering behavior was examined under two primary conditions: (1) high-temperature, short-duration tempering (>200°C, <30 seconds), and (2) low-temperature, long-duration tempering (around 200°C, >5 minutes).

3. RESULTS AND DISCUSSION

CCT diagram from dilatometer simulations, as shown in Figure 3, indicates that the critical cooling rate for achieving a martensitic transformation was 16°C/s, with a Ms temperature of approximately 340°C. To ensure the formation of a fully martensitic structure while maintaining a sufficient cooling margin, a cooling rate above 20°C/s was selected for simulations. Three distinct experimental conditions were designed to investigate the influence of thermal parameters on the mechanical properties of the steel. These included: (1) variations in cooling rate, (2) high-temperature short-duration tempering (temperatures above 200°C with holding times less than 30 seconds), and (3) low-temperature long-duration tempering (approximately 200°C with holding times of more than 5 minutes).

Mechanical testing results from the thermal simulation experiments are summarized in Tables 1-3. Table 1 illustrates the effect of cooling rate. Reducing the cooling rate from 40°C/s to 20°C/s resulted in a slight decrease in tensile strength (approximately 30 MPa), while yield strength and elongation remained unaffected. Once martensitic transformation was completed, auto-tempering occurred, influencing the final microstructure. A slower cooling rate allowed more time for auto-tempering, which in turn led to a slight reduction in tensile strength. However, given the ultra-high strength level of the steel, the impact of cooling rate variation on overall mechanical performance is considered minimal.

Table 2 presents the effect of high-temperature short-duration tempering. Increasing the tempering temperature in the short-time regime (less than 30 seconds) led to significant strength reductions, with losses of up to 270 MPa. Elevated temperatures intensified the auto-tempering effect, substantially altering the mechanical properties.

Table 3 shows the effect of low-temperature long-duration tempering at 200°C. Prolonged tempering

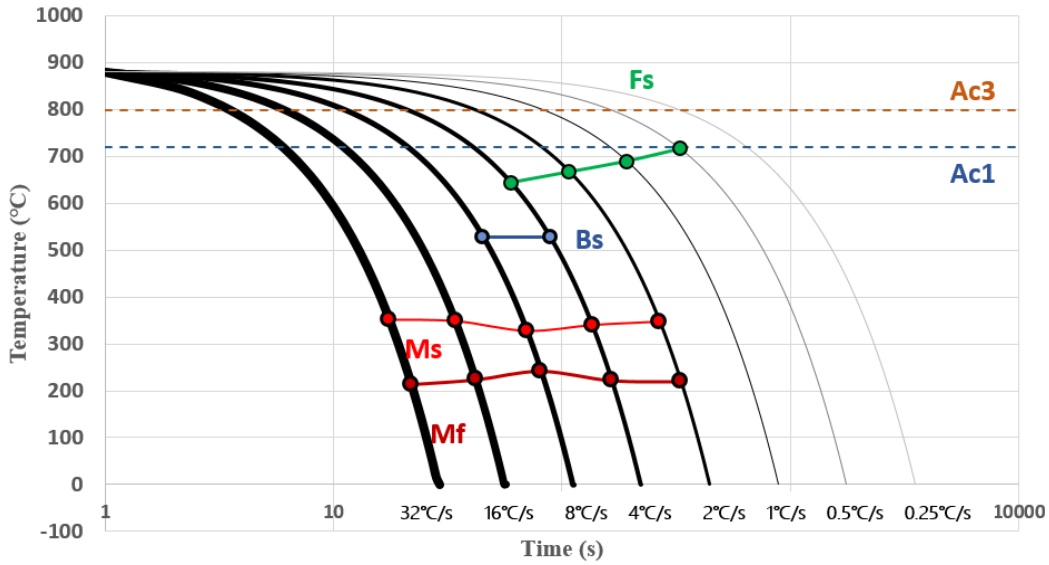

Fig.3. CCT diagram of 15B36.

Table 1 Effect of cooling rate on mechanical properties.

Cooling Rate (°C/s)	YS (MPa)	TS (MPa)	EL (%)
40	1018-1028	1772-1778	7.3-7.7
30	1027-1038	1768-1772	7.3-7.5
20	1006-1013	1741-1752	7.7-8.1

Table 2 Effect of high-temperature short-duration tempering on mechanical properties.

Temperature (°C)	Holding Time (sec)	YS (MPa)	TS (MPa)	EL (%)
260	20	1085-1094	1775-1785	7.6-7.7
280	20	1099-1105	1753-1757	6.9-7.4
300	20	1095-1109	1551-1557	7.3-7.4
320	20	1129-1131	1501-1518	6.5-6.7

Table 3 Effect of low-temperature long-duration tempering on mechanical properties.

Temperature (°C)	Holding Time (min)	YS (MPa)	TS (MPa)	EL (%)
200	5	1021-1025	1843-1855	7.4-7.6
200	10	1043-1045	1822-1826	8.0-8.1
200	20	1076-1083	1788-1791	5.8-6.4

(more than 5 minutes) resulted in strength losses of approximately 60 MPa, attributed to carbide coarsening and partial dislocation recovery over time.

Overall, the results consistently indicate that a higher degree of auto-tempering correlates with reduced tensile strength. In contrast, yield strength showed a slight increase with greater tempering intensity, while elongation remained nearly unchanged across all conditions.

Metallographic analysis provided further insight into the microstructural evolution of the steel under various heat-treatment conditions. Optical microscopy (OM) observations revealed a homogeneous microstructure predominantly composed of fine lath martensite, with no detectable presence of ferrite or retained austenite, indicating a complete martensitic transformation. Given the strong correlation between mechanical properties and the extent of auto-tempering, microstructural characterization focused on specimens subjected to the critical tempering regime, high-temperature short-duration tempering, as illustrated in Figure 4. Although all samples exhibited fully martensitic microstructures, clear differences were observed in the nature and distribution of carbide precipitates, reflecting variations in the degree of auto-tempering. At elevated tempering temperatures, carbide particles were coarser, leading to stronger etching contrast. In contrast, samples tempered at lower temperatures displayed finer carbides with reduced etching contrast, indicative of suppressed carbide coarsening and limited tempering effects. These observations suggest the sensitivity of martensitic microstructure to tempering parameters and their consequential impact on mechanical behavior.

Scanning electron microscopy (SEM) analysis, as

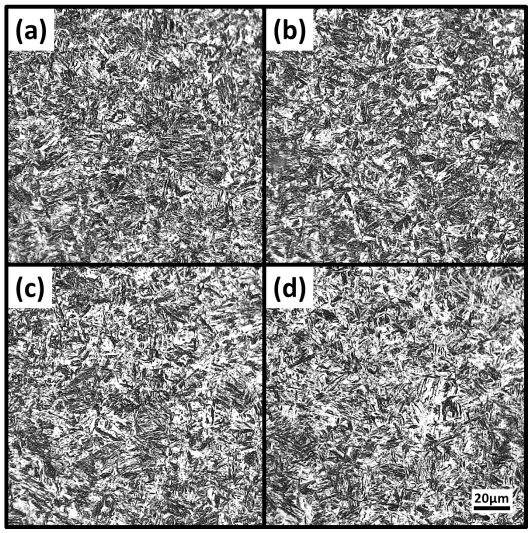

Fig.4. Optical micrograph of high-temperature short-duration tempering specimens. (a) 320℃ (b) 300℃ (c) 280℃ (d) 260℃

presented in Figure 5, revealed martensitic laths across all specimens, with no observable bainitic or ferritic phases, confirming the completion of martensitic transformation. The overall lath morphology remained consistent regardless of the applied tempering conditions, indicating structural stability within the tested thermal regime. A high-magnification SEM image, Figure 6, further disclosed the presence of fine carbide precipitates embedded within the martensitic matrix, characteristic of tempered martensite. These carbides were primarily dispersed along lath boundaries and within lath interiors, although their precise size distribution and continuity varied subtly depending on the tempering temperature.

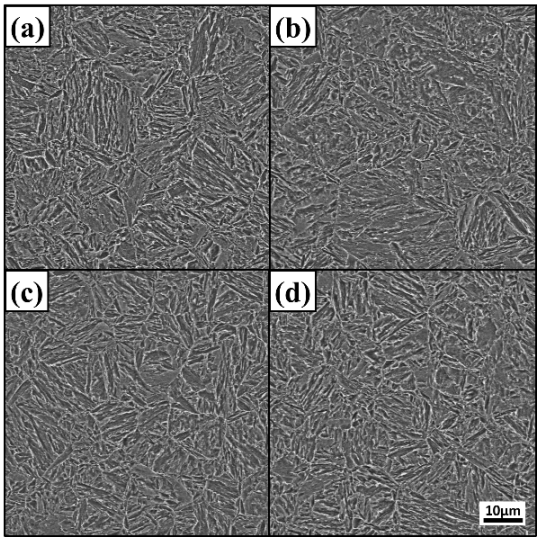

Fig.5. Low magnification SEM image of high-temperature short-duration tempering specimens. (a) 320℃ (b) 300℃ (c) 280℃ (d) 260℃

However, limitations in imaging resolution, stemming from the deep etching required to delineate martensitic features, and the restricted field of view at high magnification posed challenges in comprehensively evaluating the spatial uniformity and degree of carbide coarsening throughout the microstructure. Consequently, while localized observations suggested trends in carbide precipitation, a comprehensive quantification of carbide morphology and distribution across the entire microstructure would necessitate advanced image analysis techniques.

By electrolytic polishing, the specimen was examined by SEM under in-lens detection, as shown in Figure 6. The image clearly reveals carbide particles of varying sizes with non-uniform spatial distribution. This observation indicates differences in tempering degree between early-formed and later-formed martensite. The former exhibits more pronounced auto-tempering, while the latter appears to have undergone minimal or no tempering. Such a heterogeneous distribution of carbides is a characteristic feature of auto-tempered martensite. These microstructural features are only discernible under high-magnification SEM imaging. At lower magnifications or in macro-scale observations, the carbide distribution is not clearly visible. At present, quantitative analysis of carbide size and distribution remains challenging due to their fine scale and uneven dispersion.

These results support that the developed processing conditions effectively control martensitic transformation and tempering behavior, producing a robust microstructure and excellent mechanical performance suitable for UHSS applications.

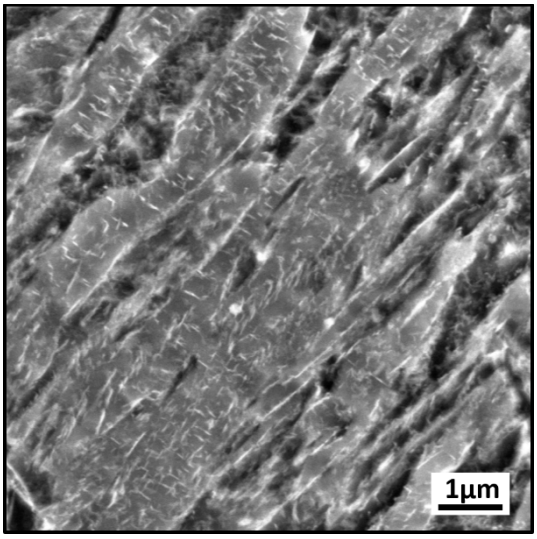

Fig.6. Fine precipitated carbides are visible in the tempered martensite under a high-magnification SEM image.

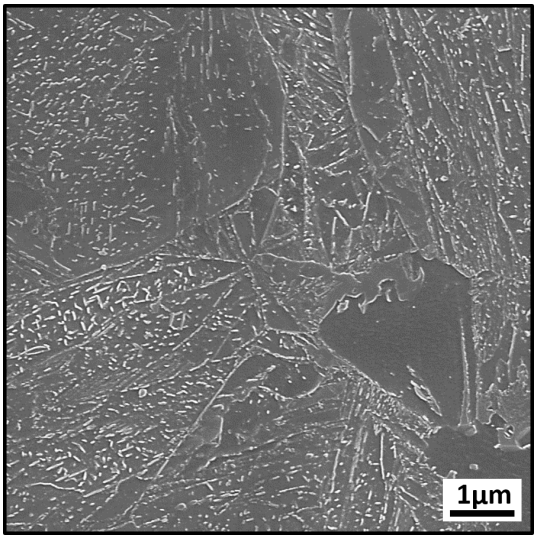

Fig.7. SEM image of auto-tempered martensite captured using in-lens detection.

4. CONCLUSIONS

This study examined the microstructures and mechanical behavior of martensitic steel using 15B36 as the base material, with particular emphasis on the influence of cooling rate and tempering conditions. Laboratory simulations revealed that reducing the cooling rate from 40°C/s to 20°C/s led to a slight decrease in tensile strength. High-temperature short-duration tempering resulted in substantial strength reductions of up to 270 MPa, whereas low-temperature long-duration tempering at 200°C caused moderate losses of approximately 60 MPa due to auto-tempering. Microstructural analysis confirmed the formation of a fully martensitic

matrix, with the degree of auto-tempering significantly affecting carbide morphology and distribution. These findings offer valuable insights for optimizing thermal processing parameters to achieve a desirable balance between strength and microstructural stability in advanced martensitic steels.

REFERENCES

1. Krauss, G., "Martensite in Steel: Strength and Structure," Materials Science and Engineering: A, vol. 273-275, 1999, pp. 40-57.
2. Chen, K.-W. et al., "Current Developments and Applications of Cold-Rolled Martensitic Steels," Automotive Materials and Industry, 2022."冷軋麻田散鐵鋼應用與開發現況," 汽車工業與材料, 2022.
3. SSAB Automotive Insights, "Advanced Martensitic Steels for Battery Protection," SSAB.com, 2023.
4. Morsdorf, L. et al. "Carbon Redistribution in Quenched and Tempered Lath Martensite," Acta Materialia: vol. 205, 2021, pp. 116521.
5. Hutchinson, B. et al. "Yielding Behaviour of Martensite in Steel," ISIJ international: vol. 55.5, 2015, pp. 1114-1122.
6. Bhadeshia, H. K. D. H., & Honeycombe, R. W. K., *Steels: Microstructure and Properties*, 4th ed., Butterworth-Heinemann, 2017.
7. Speer, J. G., Edmonds, D. V., Rizzo, F. C., & Matlock, D. K., "Partitioning of Carbon From Supersaturated Ferrite in Austenite–Ferrite Mixtures," Current Opinion in Solid State and Materials Science, vol. 8.3-4, 2004, pp. 219-237.
8. Koistinen, D. P., & Marburger, R. E., "A General Equation Prescribing the Extent of the Austenite-Martensite Transformation in Pure Iron-Carbon Alloys and Plain Carbon Steels," Acta Metallurgica, vol. 7, no. 1, 1959, pp. 59-60.